Int. J. Electrochem. Sci., 10 **(2015)** 2014 - 2025

International Journal of
ELECTROCHEMICAL
SCIENCE
www.electrochemsci.org

Effect of Cerium Acetate Doping on Corrosion Behavior of Sol-Gel Coatings on 2A12 Aluminum Alloy

Chunjuan Fu[*], *Yuxing Liu, Mei Yu, Jianhua Liu, Songmei Li*

School of Materials Science and Engineering, Beihang University, Beijing, 100191, China
[*]E-mail: fuchunjuan@buaa.edu.cn

Received: 26 November 2014 / *Accepted:* 4 January 2015 / *Published:* 19 January 2015

Si-Zr hybrid sol-gel coatings on 2A12 aluminum substrate were prepared, and the effect of cerium acetate ($Ce(CH_3COO)_3$) doping on corrosion behavior of the sol-gel coatings was examined. The scanning electron microscopy (SEM) was employed to investigate the morphology of the coatings, and the corrosion resistance of the coatings was evaluated by electrochemical methods and neutral salt spray tests. In addition, the structure and the inhibition mechanism of $Ce(CH_3COO)_3$ doped sol-gel coatings were discussed by Fourier transform infrared (FTIR) analysis. It is indicated that proper doping concentration of $Ce(CH_3COO)_3$ can effectively improve the corrosion resistance of the sol-gel coatings, while the higher concentration of $Ce(CH_3COO)_3$ would reduce the homogeneity and stability of the coatings, and further destroy the corrosion protection properties of the coatings.

Keywords: $Ce(CH_3COO)_3$ doping; Sol-gel; Coatings; Corrosion protection

1. INTRODUCTION

Aluminum alloys have been extensively used in many fields including aeronautics, building and automotive industry et al. Thereinto, the alloy 2A12 is paid special attention with its remarkable mechanical strength and low density [1]. However, the high Cu content makes 2A12 susceptible to pitting corrosion, intergranular corrosion and even exfoliation corrosion [2]. Therefore, it is important to prevent or retard corrosion of 2A12 by applying protective coatings.

At the moment, as a viable alternative to chromates, sol-gel based coatings have been successfully deposited on the alloy 2A12 and exhibit superior protective performance to severe environment [3-5]. The hydrolyzable inorganic part in the sol-gel coatings can form stable covalent bond with the metal substrate, which increases the binding force, thermal stability and mechanical properties of the coatings. On the other hand, the organic part can participate in the corresponding characteristic reaction with functional group and produce crosslinked structure, which makes the

coatings more flexible and hydrophobic [4, 6-8]. The Si-Zr hybrid sol-gel coatings used in present study are homogeneous multiphase coatings, and have been widely studied and applied in improving the corrosion resistance of 2A12 aluminum alloy and other metal. However, due to the lack of self-healing property, the sol-gel coatings cannot stop the development of corrosion process when the defects appear. To solve this problem, corrosion inhibitors were introduced into sol-gel coatings.

Among various corrosion inhibitors, cerium salts are considered to be a good type of environmentally friendly corrosion inhibitors [9-13]. Corrosion protection offered by the cerium-containing coatings is mainly achieved by the obstruction of the cathodic oxygen reduction reaction [14]. Some authors [15, 16] proposed that cerium ions can substitute some of the Si atoms in the coatings, leading to the formation of a modified Si-O-Ce network. In addition, it was reported that a combination of different inhibiting species such as rare earth elements with organic acid groups can provide a synergistic inhibition effect [16], consequently confer a superior corrosion inhibition for alloys. Cerium phosphates [18], cerium cinnamate [19] and cerium silicate [20] were tested as inhibitors and exhibited promising corrosion resistance. However, the addition of the cerium salt would result in some side effects, such as reduced stability, homogeneity and smoothness of sol-gel, moreover, some inhibitors are not easily controlled due to rapid release from the coatings [21]. In addition, the solubility of the inhibitor has significant effect on the long-term corrosion protection properties of sol-gel coatings [22]. Therefore, it is important to explore the optimal inhibitor concentration. To this end, Si-Zr hybrid sol-gel coatings doped with different concentrations of $Ce(CH_3COO)_3$ on 2A12 aluminum alloy were prepared, and the effects of $Ce(CH_3COO)_3$ concentration on the morphology, structure and corrosion resistance of the coatings were examined. The inhibition mechanism of $Ce(CH_3COO)_3$ was discussed.

2. EXPERIMENTAL

2.1. Pretreatment of substrate

The nominal composition of aluminum alloy 2A12 was given in Table 1. Before deposition, the alloy was cut into rectangular panel samples with dimensions of 40 mm × 30 mm × 2 mm. Then the samples were mechanically abraded with abrasive papers up to grit #800, and pretreated successively by means of alkaline cleaning, alkaline etching and acid desmutting. Finally, the samples were rinsed in water and dried in air.

Table 1. Nominal composition of 2A12 aluminum alloy

Element	Concentration (wt.%)
Cu	3.8-4.9
Mg	1.2-1.8
Mn	0.3-0.9
Zn	0.25
Si	0.5
Fe	0.5
Al	Balance

2.2. Preparation of the coatings

The coatings were prepared by sol-gel technology. Concurrently, two separate sols, a Si sol and a Zr sol, were formulated. The Si sol was prepared by mixing glycidoxypropyl-trimethoxy-silane (GTMS, analytical, Nanjing Capatue Chemical Co., Ltd, China) with ethanol of equal volume. Distilled water was dropwise added to enable hydrolysis of GTMS while continuously stirring the solution, and the molar quantity of the distilled water was one third of ethanol. For the Zr sol, Zirconium (IV) n-propoxide (TPOZ, 70% w/w in n-propanol, Alfa Aesar), ethyl acetoacetate, and ethanol were used as the source of hydrolysable zirconium, the catalyst, and the solvent, respectively. TPOZ was independently chelated with ethanol and ethyl acetoacetate in volume ratio of 8:12:3. Both of the two sol solutions were stirred for 1 h in sealed beakers, and then the Zr sol was gently added into the Si sol with stirring. The molar ratio of Si to Zr in mixed solution was 3:1. Afterwards the mixed solution was sealed and kept on stirring for 3 h. Finally, different concentrations of $Ce(CH_3COO)_3$ were added, following by stirring for 1 h. The concentrations of $Ce(CH_3COO)_3$ were 0.001 M, 0.005 M, 0.01 M and 0.05 M, respectively.

The coatings were deposited on 2A12 samples by dip-coating with a withdraw speed of 10 cm/min for two times. The time of each immersion into the solution was 5 min. Between the two immersions, the samples were dried in air for 15 min. After the second immersion, the samples were cured at 60 °C for 3 h, 90 °C for 1 h, and 120 °C for 0.5 h in an oven.

2.3. Characterizations

Sol-gel coatings with different concentrations of $Ce(CH_3COO)_3$ were analyzed by using a scanning electron microscope (SEM, Apollo 300, Cam Scan, Britain) to investigate the morphology of coatings.

The electrochemical tests were carried out by using an Advanced Electrochemical System (PARSTAT 2273, Princeton, USA). A three-electrode cell was employed, consisting of a saturated calomel reference electrode (SCE), a platinum foil as counter electrode, and the coated samples as working electrode with a surface area of 1 cm^2. The test solution was 0.05 M NaCl solution. The electrochemical impedance spectroscopy (EIS) measurements were conducted with AC excitation amplitude of 10 mV at open circuit potential. The frequency range was from 100 kHz to 10 mHz with 50 data points per decade. Before each measurement, the coated samples were immersed into the NaCl solution for 30 min until they reached a steady state. All the spectra were recorded at open circuit potential (OCP). In order to ensure reproducibility of the measurements, the samples were tested in triplicate.

The corrosion resistance of the coated samples was examined by putting them into a salt spray chamber (WYX/Q-250, YaShiLin, China). The spray solution was 5 wt.% NaCl solution (pH 6.5-7.2). The temperature was kept at 35°C, and the angle of the tested surface was set at 20°.

The Fourier transform infrared (FTIR) measurements of the coatings were performed on a Thermo Nicolet Nexus 470 Fourier transform spectrometer. The spectra were averages of 32 scans, and the range of FTIR spectra was about 500-4000 cm^{-1}.

3. RESULTS AND DISCUSSION

3.1. Morphology of the coatings

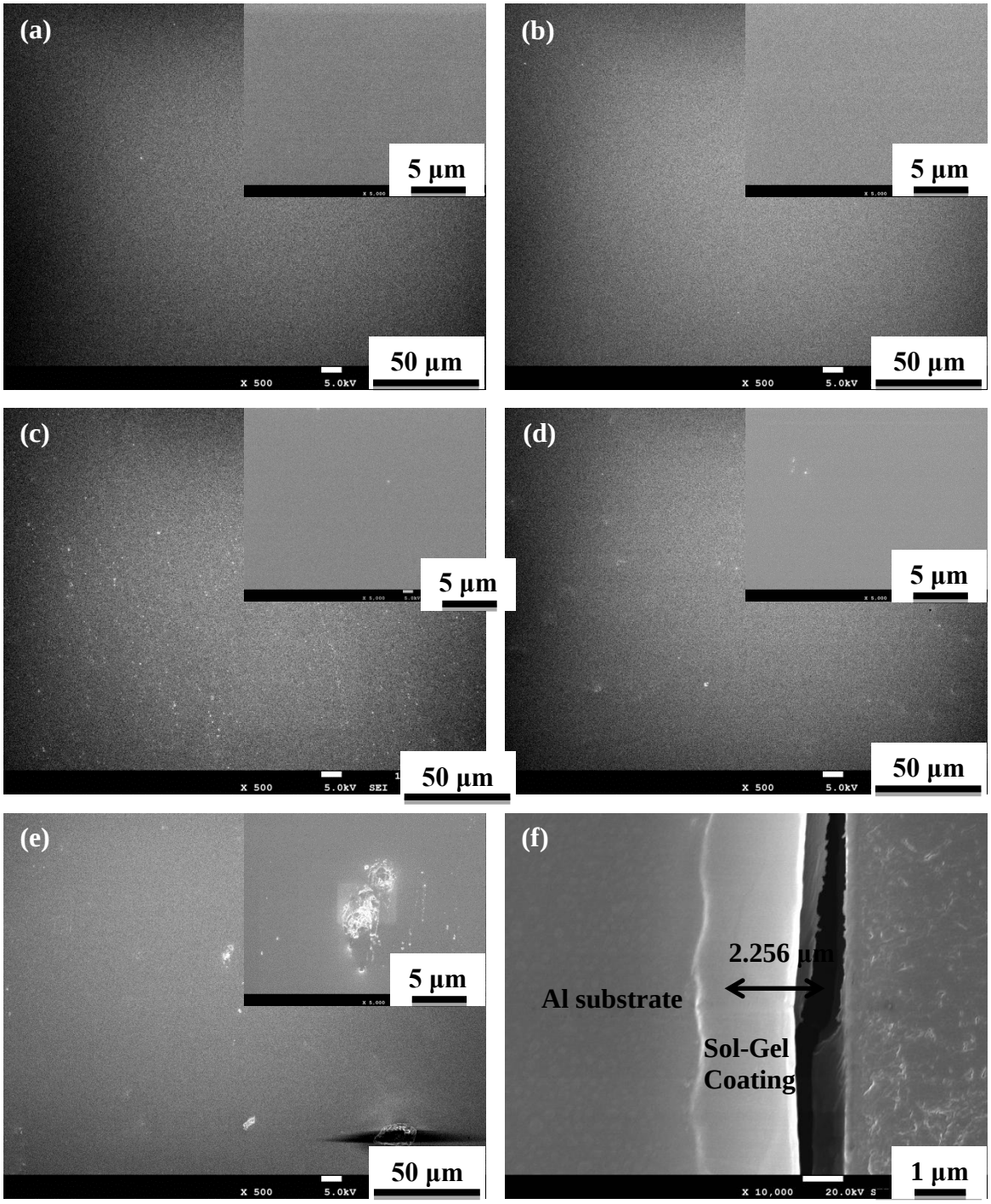

Figure 1. SEM images of different coatings. (a) undoped, (b) 0.001 M doped, (c) 0.005 M doped, (d) 0.01 M doped, (e) 0.05 M doped, (f) cross sections of 0.01 M $Ce(CH_3COO)_3$ doped.

The SEM images of different coatings are shown in Fig. 1. The coatings without and with 0.001 M $Ce(CH_3COO)_3$ are flat and smooth, and no crack or pinhole is observed even when it was

enlarged to a magnification of 5000, as shown in Fig. 1(a, b). By comparison, the coatings doped with 0.005 M and 0.01 M show poor flatness in local area (Fig. 1(c, d)). However, the coatings can still cover the alloy surface completely without affecting the integrity. From Fig. 1(e), it can be seen that the coating doped with 0.05 M $Ce(CH_3COO)_3$ shows some tiny defects. The magnified image reveals the appearance of agglomeration, which may be attributed to the cladding capacity of coating for external particles. It is known that the inclusion of bigger Ce cations into the sol will induce partial destabilization of the sol-gel network and consequently affect the property of coating [12]. The cross section of 0.01 M $Ce(CH_3COO)_3$ doped coating is shown in Fig. 1(f). It can be seen that the coating is tightly adhered to the surface of 2A12 aluminum substrate, and no obvious separated layer is detected within the coating. This phenomenon indicates that the double dip-coating does not influence the adherence between the two layers.

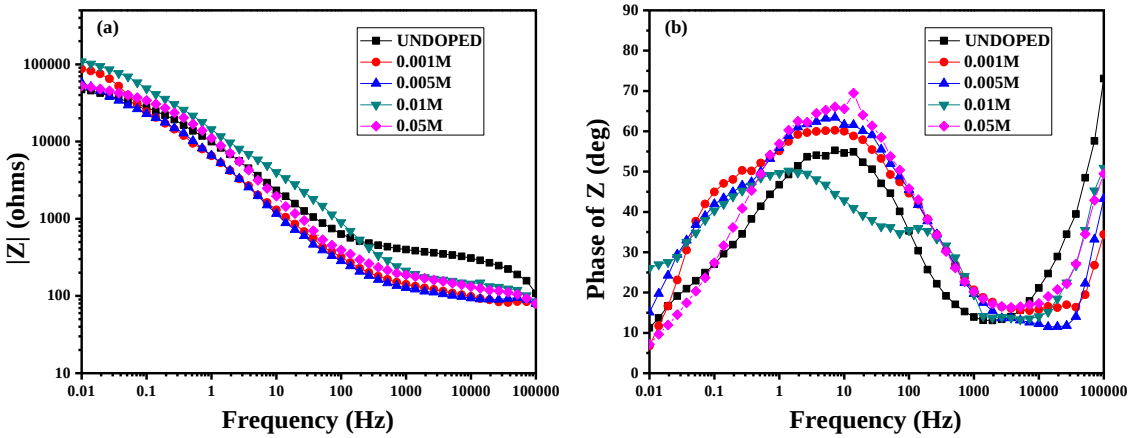

Figure 2. EIS of different sol-gel coatings immersed in 0.05 M NaCl solution for 1 h

3.2. Corrosion resistance of the coatings

3.2.1. Electrochemical impedance spectroscopy: immersion tests

The Bode plots of different sol-gel coatings obtained after immersion for 1 h in 0.05 M NaCl solution are presented in Fig. 2. All the impedance curves have the similar trend that the impedance values of coatings increase with the decrease of frequency. Low-frequency impedance values reflect the overall resistance of sol-gel coatings [23]. Comparing with the other coatings, the coating doped with 0.01 M $Ce(CH_3COO)_3$ presents the highest low-frequency impedance value which means the best barrier properties. The phase plots show two well defined time constants at the initial stage of immersion. The one at high frequency (around 10^5 Hz) is attributed to the relaxation process of the external organic layer and the other time constant at lower frequency results from the inorganic oxide layer between the metal surface and sol-gel coating.

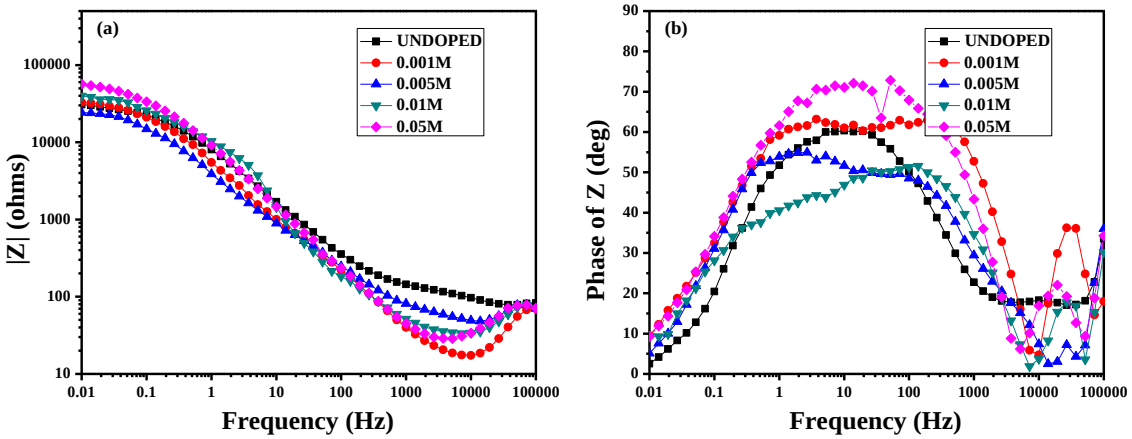

Figure 3. EIS of different sol-gel coatings immersed in 0.05 M NaCl solution for 24 h

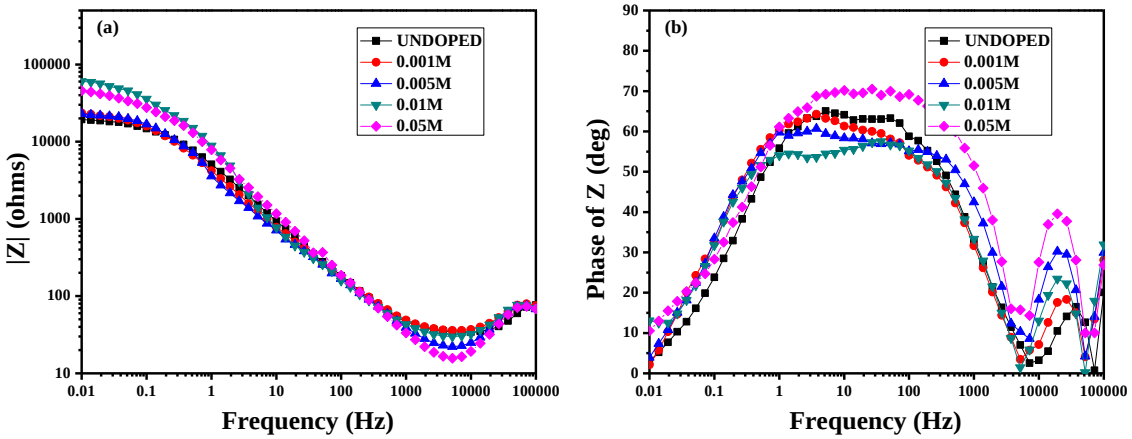

Figure 4. EIS of different sol-gel coatings immersed in 0.05 M NaCl solution for 72 h

Fig. 3 presents the Bode plots of different sol-gel coatings after immersion for 24 h in 0.05 M NaCl solution. It is observed that the impedance values of the coatings at low frequency decrease significantly. The phase angles of the time constant at high frequency decrease by about 20 degrees, which indicates that electrolyte and water probably have penetrated through the organic layers and begin to attack the oxide layers. The low-frequency impedance value of the coating without $Ce(CH_3COO)_3$ keeps on decreasing after immersion for 72 h, while it increases in varying degrees for the coatings doped with different concentrations of $Ce(CH_3COO)_3$, as shown in Fig. 4. The increase of the impedance values is attributed to the self-healing effect of inhibitor [24]. The low-frequency impedance value of coating doped with 0.01 M $Ce(CH_3COO)_3$ increases the most, indicating that the coating has significantly better barrier properties and higher stability against electrolytic attack. The phase angles of the time constant at high frequency continue to decrease, indicating that the corrosive medium has permeated abundantly, and the corrosion mechanism began to change. In addition, the phase angles at high frequency (10^4-10^5Hz) generally increase with the increase of content of

$Ce(CH_3COO)_3$, indicating that $Ce(CH_3COO)_3$ can maintain the compactness of the external structure of the organic layer effectively.

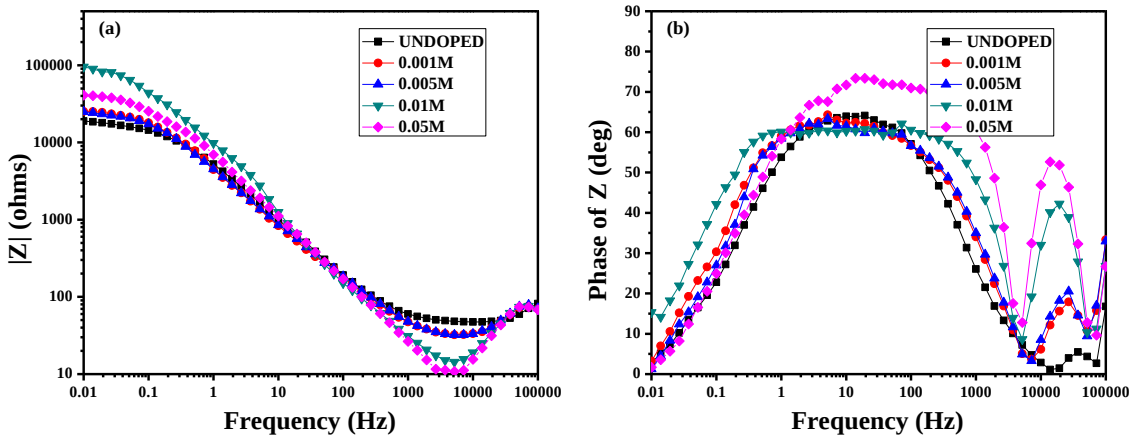

Figure 5. EIS of different sol-gel coatings immersed in 0.05 M NaCl solution for 168 h

The Bode plots of different sol-gel coatings after immersion for 168 h in 0.05 M NaCl solution are shown in Fig. 5. It is clearly seen that low-frequency impedance value of the coating without $Ce(CH_3COO)_3$ doped keeps on decreasing, while the coatings with $Ce(CH_3COO)_3$ doped exhibit higher low-frequency impedance. And the coating doped with 0.01 M $Ce(CH_3COO)_3$ presents the highest low-frequency impedance value. In addition, the phase angles of time constant at low frequency increase remarkably for all coatings doped with $Ce(CH_3COO)_3$, indicating that oxides of cerium have formed.

3.2.2. Potentiodynamic polarization curves

The polarization curves of different sol-gel coatings immersed in 0.05 M NaCl solution for 14 days are shown in Fig. 6. It can be seen that all of the coatings doped with $Ce(CH_3COO)_3$ have lower current density than the undoped one, which indicates a stronger corrosion resistance when adding $Ce(CH_3COO)_3$ into the coatings. Moreover, the corrosion potential increases with the concentration of $Ce(CH_3COO)_3$ in the range from 0.001 M to 0.01 M, showing a gradual increase in the corrosion resistance of coatings. The coating doped with 0.01 M $Ce(CH_3COO)_3$ exhibits the most positive corrosion potential and a slight decrease in the current density, indicating a modified protection ability. For the coating doped with 0.05 M $Ce(CH_3COO)_3$, the corrosion potential decreases, which indicates that an excess of $Ce(CH_3COO)_3$ would reduce the corrosion resistance of the coating. This phenomenon can be associated with the nonuniform and defective morphology presented in Fig. 1(e).

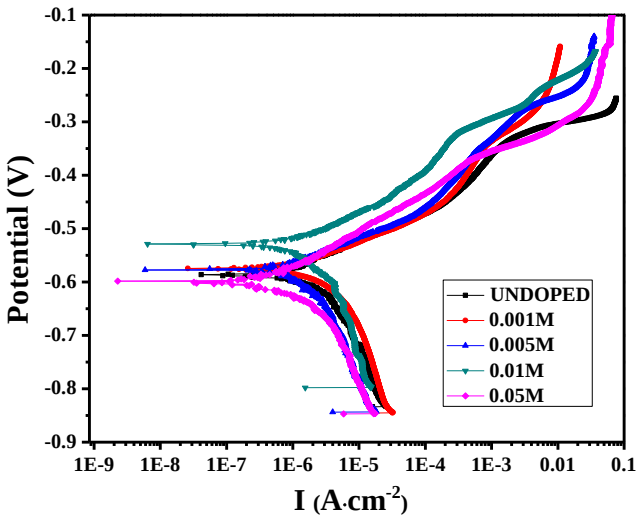

Figure 6. Potentiodynamic polarization curves of different sol-gel coatings after immension for 14 d.

Some kinetic parameters such as the corrosion potential (E_{corr}), the corrosion current density (j_{corr}), the slope of anodic curve (b_a) and cathodic curve (b_c), the polarization resistance (R_p) and *corrosion rate* are listed in Table 2. The E_{corr} and j_{corr} are derived by extrapolating the linear portions of the polarization curves in Figure 6. R_p was derived by the equation $R_p = \frac{1}{2.3 \cdot j_{corr}} \left(\frac{b_a \cdot b_c}{b_a + b_c} \right)$ [29, 30], and the *corrosion rate* for the coatings was calculated by using the equation $Corrosion\ rate = \frac{0.13 \times j_{corr} \times E.W}{d}$, where *E.W* is the equivalent weight of the metal (Al) which is 9 g and *d* is the density of the corroding species (2.78 g·cm^{-3}) [31, 32]. It can be observed that all the coatings doped with $Ce(CH_3COO)_3$ present a lower corrosion current density comparing with the undoped coating. Among them, the coating doped with 0.01 M $Ce(CH_3COO)_3$ possesses the highest E_{corr} and R_p.

Table 2. Electrochemical parameters derived from polarization curves of different sol-gel coatings

	E_{corr} (mV)	j_{corr} (A·cm^{-2})	b_a (V·dec^{-1})	b_c (V·dec^{-1})	R_p (Ω·cm^{-2})	*Corrosion rate* (mpy)
UNDOPED	-565.3	1.59×10^{-6}	0.05	0.19	1.082×10^{4}	0.6692
0.001M	-561.9	1.39×10^{-6}	0.05	0.11	1.075×10^{4}	0.5850
0.005M	-563.3	8.09×10^{-7}	0.05	0.13	1.941×10^{4}	0.3404
0.01M	-533.5	8.26×10^{-7}	0.06	0.10	1.974×10^{4}	0.3476
0.05M	-566.0	1.17×10^{-6}	0.07	0.13	1.691×10^{4}	0.4924

3.2.3. Salt spray tests

The neutral salt spray test is applied to evaluate the corrosion resistance of the coated 2A12 aluminum substrates in severe environment. The optical images of different samples after 96 h

exposure in 5 wt.% NaCl neutral salt spray chamber are shown in Fig. 7. The bare 2A12 aluminum substrate in Fig. 7(a) is badly damaged, and the coated sample without $Ce(CH_3COO)_3$ in Fig. 7(b) shows a large number of pitting sites across the surface. Tiny pitting corrosion is also observed for coating doped with 0.05 M $Ce(CH_3COO)_3$ in Fig. 7(f). As expected, no pitting is detected on the surface of coating in Fig. 7(c-e), especially the 0.01 M $Ce(CH_3COO)_3$ doped one. In short, the coatings doped with moderate $Ce(CH_3COO)_3$ exhibit improved corrosion protection after 96 h exposure in neutral salt spray chamber, which is in agreement with the results of immersion tests.

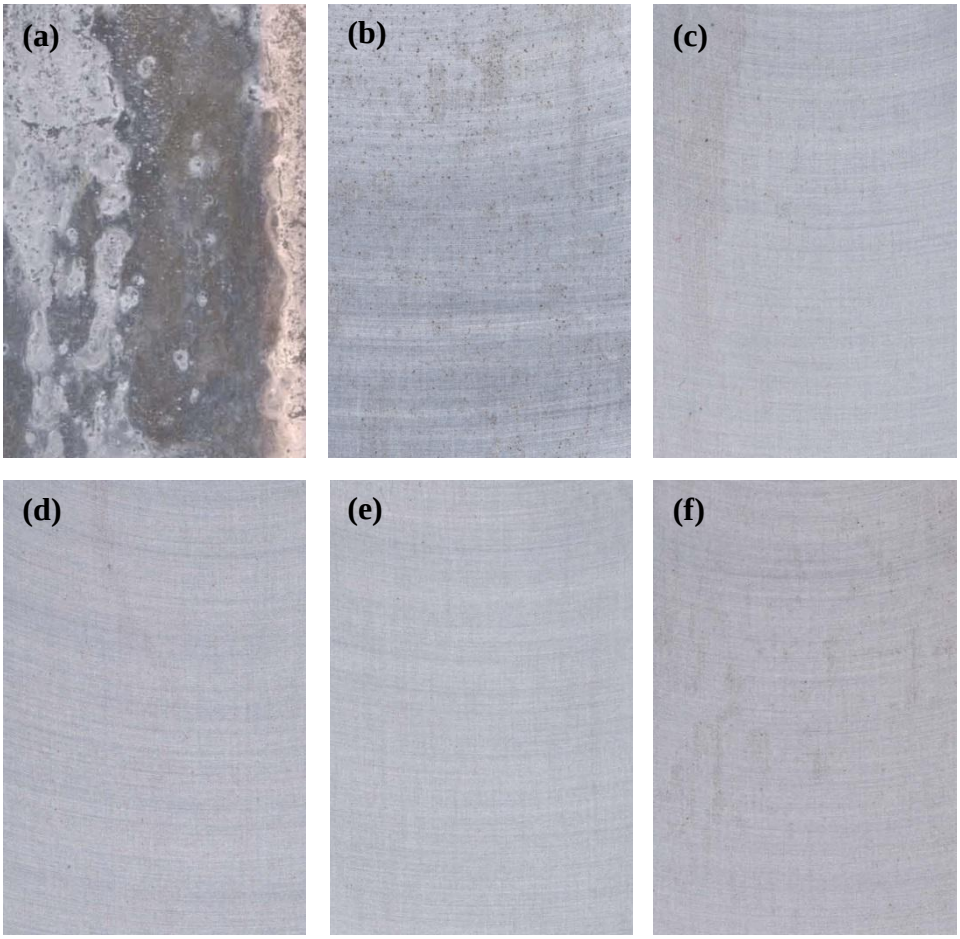

Figure 7. Photos of various samples after 96 h exposure in salt-spray chamber. (a) bare 2A12 sample, (b) coated sample without $Ce(CH_3COO)_3$, (c) 0.001 M doped, (d) 0.005 M doped, (e) 0.01 M doped, (f) 0.05 M doped.

Based on the above analysis of morphology and corrosion resistance of the sol-gel coatings, the optimal concentration of $Ce(CH_3COO)_3$ is 0.01 M. In this case, the coating is uniform, dense and full coverage, and presents the best corrosion resistance in this study.

3.3. Inhibition mechanism of $Ce(CH_3COO)_3$

The FTIR transmittance spectra for different sol-gel coatings deposited on 2A12 samples are shown in Fig. 8. To get a full and detailed vision, the spectra were broken at 1800 cm^{-1} and divided into two parts with different wavenumber increments.

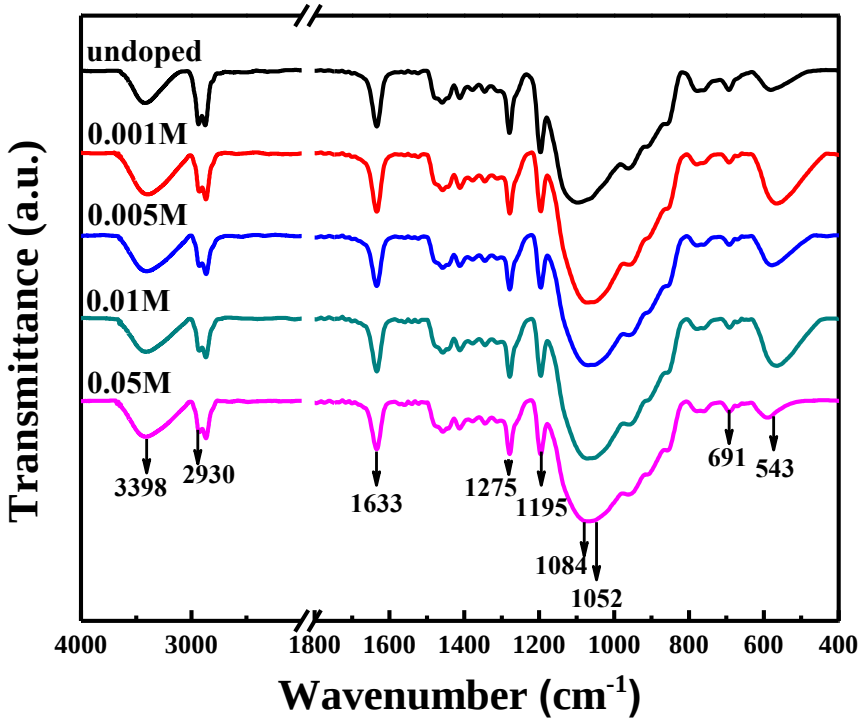

Figure 8. Infrared spectra of 2A12 coated with different sol-gel coatings

For all the sol-gel coatings, two peaks at 1084 cm^{-1} and 1052 cm^{-1} are noticeable, which are assigned to Si-O-Si stretching vibration in cage and network configurations formed by the condensation reaction of silanol [25, 26]. Small peaks observed at 1633 cm^{-1} correspond to the Si-O-Zr bonds [27]. It is concluded that a hybrid network containing zirconia and organo-silica is formed in the sol-gel coatings. The peak around 1275 cm^{-1} is attributed to the vibration of epoxy groups [28]. The intensity of this peak for the coatings doped with $Ce(CH_3COO)_3$ is slightly lower than the undoped one, indicating that ring opening reactions have happened during the deposition of GTMS. Besides, the ring opening reactions enhance with the increase of the concentration of $Ce(CH_3COO)_3$. The coatings doped with 0.001 M, 0.005 M, 0.01 M $Ce(CH_3COO)_3$ present higher intensity at 543 cm^{-1}, which is due to C-H out of plane deformation of aromatic ring of epoxy resin. The result indicates that moderate $Ce(CH_3COO)_3$ is in favor of ring opening reaction and thus forming a dense three-dimensional network structure. However, the peak intensity of the coating doped with 0.05 M $Ce(CH_3COO)_3$ decreases at 543 cm^{-1}, indicating that an excess of $Ce(CH_3COO)_3$ will hinder the formation of a dense network structure in the coating. This phenomenon well explains above test results of corrosion resistance and confirms the better corrosion protective performance promoted by 0.01 M $Ce(CH_3COO)_3$.

4. CONCLUSIONS

Proper doping concentration of $Ce(CH_3COO)_3$ can effectively improve the corrosion resistance of sol-gel coatings without affecting the integrity of the coatings. However, an excess of $Ce(CH_3COO)_3$ (0.05 M) would reduce the corrosion resistance of the coating, which is associated with the nonuniform and defective morphology. The optimal concentration of $Ce(CH_3COO)_3$ is 0.01 M. In this case, the coating is uniform, dense and full coverage, and has significantly better barrier properties and higher stability against electrolytic attack.

It is shown that moderate $Ce(CH_3COO)_3$ is in favor of ring opening reaction and thus forming a dense three-dimensional network structure, and further increasing the compactness of external structure of the organic layer. Oppositely, an excess of $Ce(CH_3COO)_3$ will hinder the ring opening reaction and reduce the corrosion resistance of the coating eventually.

ACKNOWLEDGEMENTS
This work was supported by Aero Science Foundation of China (No. 2011ZE51057) and the Fundamental Research Funds for the Central Universities.

References

1. E.A. Starke and J.T. Staley, *Prog. Aerospace Sci.*, 32 (1996) 131.
2. N. Voevodin, C. Jeffcoate, L. Simon, M. Khobaib and M. Donley, *Surf. Coat. Technol.*, 140 (2001) 29.
3. J.F. Huang, *The Principle and Technology of Sol-Gel*, Chemical Industry Press, Beijing (2005).
4. J.H. Liu, L. Dong, M. Yu, S.M. Li and Z.W. Zhan, *Acta Chim. Sinica*, 70 (2012) 2179.
5. C.J. Fu, Z.W. Zhan, M. Yu, S.M. Li, J.H. Liu and L. Dong, *Int. J. Electrochem. Sci.*, 9 (2014) 2603.
6. D. Wang and G.P. Bierwagen, *Prog. Org. Coat.*, 64 (2009) 327.
7. Z. Feng, Y. Liu, G.E. Thompson and P. Skeldon, *Electrochim. Acta*, 55 (2010) 3518.
8. T. L. Metroke, O. Kachurina and E. T. Knobbe, *Prog. Org. Coat.*, 44 (2002) 295.
9. B.R.W. Hinton, *J. Alloys Compd.*, 180 (1992) 15.
10. A.J. Aldykiewicz Jr., A.J. Davenport and H.S. Isaacs, *J. Electrochem. Soc.*, 143 (1996) 147.
11. R.Z. Zand, K. Verbeken and A. Adriaens, *Int. J. Electrochem. Sci.*, 8 (2013) 548.
12. D. Raps, T. Hack, J. Wehr, M.L. Zheludkevich, A.C. Bastos, M.G.S. Ferreira and O. Nuyken, *Corros. Sci.*, 51 (2009) 1012.
13. M.L. Zheludkevich, S.K. Poznyak, L.M. Rodrigues, D. Raps, T. Hack, L.F. Dick, T. Nunes and M.G.S. Ferreira, *Corros. Sci.*, 52 (2010) 602.
14. A.K. Mishra and R. Balasubramaniam, *Corros. Sci.*, 49 (2007) 1027.
15. M. F. Montemor and M. G. S. Ferreira, *Electrochim. Acta*, 52 (2007) 7486.
16. A. Yabuki, A. Kawashima and I.W. Fathona, *Corros. Sci.*, 85 (2014) 141.
17. A. Yurt, G. Bereket and C. Ogretir, *J. Mol. Struct.: THEOCHEM*, 725 (2005) 215.
18. T.A. Markley, M. Forsyth and A.E. Hughes, *Electrochim. Acta*, 52 (2007) 4024.
19. H. Shi, E.H. Han and F. Liu, *Corros. Sci.*, 53 (2011) 2374.
20. P.A. White, A.E. Hughes, S.A. Furman, N. Sherman, P.A. Corrigan, M.A. Glenn, D. Lau, S.G. Hardin, T.G. Harvey, J. Mardel, T.H. Muster, S.J. Garcia, C. Kwakernaak and J.M.C. Mol, *Corros. Sci.*, 51 (2009) 2279.
21. X.D. He and X.M. Shi, Self-repairing coating for corrosion protection of aluminum alloys: a proof-of-concept using cagelike smart particles [C], *Transportation Research Board 87th Annual*

Meeting (2008).
22. V. Moutarlier, B. Neveu and M.P. Gigandet, *Surf. Coat. Technol.*, 202 (2008) 2052.
23. V. Palanivel, D. Zhu and W.J. van Ooij, *Prog. Org. Coat.*, 47 (2003) 384.
24. H. Shi, F.C. Liu and E.H. Han, *Mater. Chem. Phys.*, 124 (2010) 291.
25. M.S. Oliver, K.Y. Blohowiak and R.H. Dauskardt, *J. Sol-Gel Sci. Technol.*, 55 (2010) 360.
26. E.S. Park, H.W. Ro, C.V. Nguyen, R.L. Jaffe and D.Y. Yoon, *Chem. Mater.*, 20 (2008) 1548.
27. L. Armelao, S. Gross, K. Müller, G. Pace, E. Tondello, O. Tsetsgee and A. Zattin, *Chem. Mater.*, 18 (2006) 6019.
28. J. Kim, P.C. Wong, K.C. Wong, R.N.S. Sodhi and K.A.R. Mitchell, *Appl. Surf. Sci.*, 253 (2007) 3133.
29. R.G. Kelly, J.R. Scully, D.W. Shoesmith and R.G. Buchheit, *Electrochemical Techniques in Corrosion Science and Engineering*, CRC Press (2002).
30. I.A. Kartsonakis, E.P. Koumoulos, A.C. Balaskas, G.S. Pappas, C.A. Charitidis and G.C. Kordas, *Corros. Sci.*, 57 (2012) 56.
31. M.A. Quraishi, M.Z.A. Rafiquee, S. Khan and N. Saxena, *J. Appl. Electrochem.*, 37 (2007) 1153.
32. R.V. Lakshmi, G. Yoganandan, K.T. Kavya and B.J. Basu, *Prog. Org. Coat.*, 76 (2013) 367.